

# A practical approach to flexibility provision assessment in an unobservable distribution network

Martin Bolfek<sup>a,\*</sup>, Tomislav Capuder<sup>b</sup>

<sup>a</sup> Croatia Distribution System Operator (HEP ODS), Koprivnica, Croatia

<sup>b</sup> Faculty of Electrical Engineering and Computing, University of Zagreb, Croatia

## ARTICLE INFO

### Keywords:

Optimization

Flexibility provision

Limited network observability

## ABSTRACT

Growing number of controllable generation, load and storage in distribution networks, have created an opportunity for ancillary services provision to the network operators to more effectively manage everyday grid operation, flexibility provision being one such service. The system operator's role is to exploit this service effectively while ensuring no grid constraints will be violated. This is often precluded by the lack of measurements deployed in a typical distribution grid. This paper develops a deterministic, optimization-based approach to pre-detect the permissible range of nodal flexibility provision in a distribution network with limited observability where only ranges of nodal power injections are known. Feasibility for the entire permissible range of flexibility with respect to network voltage constraints is ensured by design. Furthermore, we identify and describe a problem stemming from having multiple flexibility providers that influence each others' ability to provide the service. The method is extended to aggregating the flexibility where special attention is given to establishing fairness among the service providers. We test the efficacy of the proposed method on a modified IEEE 33 and three real world distribution networks.

## 1. Introduction

In order to limit the evermore increasing effects of climate change a complete decarbonization of energy sector is needed. Variable renewable energy sources (VRES), characterized by uncertainty, will likely play a key role in this process. This variability, as well as issues arising from the electrification of other energy sectors could be partly mitigated by flexibility provision — the technical ability to change grid user's power consumption or generation upon request [1]. As shown recently in [2], flexibility will likely play a key role in mitigating the undesirable effects of VRES on every day grid operations. In an effort to increase the rate of adoption of VRES, market based frameworks for flexibility provision, focused on the grid user, are being established. This represents an operational paradigm shift for distribution system operators (DSO), where additional opportunities for a more effective grid operation occur simultaneously with an increase in its complexity. The DSOs are expected to operate the grid in the most efficient manner possible, while at the same time enabling high VRES penetration and creating conditions for aggregators' distribution and/or transmission level market participation. However, as pointed out in recent European DSO statistics report [3], most of DSOs lack measurement data that would make their networks fully observable. This makes it difficult to verify if the network constraints are being violated in real time,

which forces the DSO to be overly cautious in both planning and day to day grid operations resulting in grid overbuilding and sub-optimal grid management strategies.

The objective of this paper is to establish a method to determine the permissible range of flexibility that can be provided by a flexibility provider (FP) at a specific node in a distribution network (DN) with limited observability. We define a flexibility provider as a grid user that is able and willing to change its power consumption/generation in order to provide some form of service to system operators in order for them to manage the system in a more efficient manner (i.e. alleviate congestion, provide tertiary reserve, reduce voltage issues, etc.). The proposed method aims to pre-detect FP's operational regimes which do not violate the voltage constraints of the DN regardless of the realization of unknown power and substation voltage fluctuations.

A number of papers have already discussed this issue ([4–9]), most of them implicitly through various implementations of TSO-DSO coordination schemes, where a DN capability curve is formed which can then be utilized by the transmission system operator (TSO). Most of these approaches, however, assume full DN observability. Several recent papers [10–12] do address the issue of limited observability, but these methods either cannot ensure the feasibility of the entire range

\* Corresponding author.

E-mail addresses: [martin.bolfek@hep.hr](mailto:martin.bolfek@hep.hr) (M. Bolfek), [tomislav.capuder@fer.hr](mailto:tomislav.capuder@fer.hr) (T. Capuder).

<https://doi.org/10.1016/j.epsr.2022.108262>

Received 15 December 2021; Received in revised form 1 June 2022; Accepted 1 July 2022

Available online 19 July 2022

0378-7796/© 2022 The Authors. Published by Elsevier B.V. This is an open access article under the CC BY license (<http://creativecommons.org/licenses/by/4.0/>).

## Nomenclature

### Sets

$N$	The set of nodes in the network
$N_{sl}$	The set of slack nodes
$N_g$	The set of distributed generator nodes
$N_d$	The set of nodes with loads
$N_{fl}$	The set of nodes with flexibility providers
$E$	The set of <i>from</i> edges in the network
$E^R$	The set of <i>to</i> edges in the network

### Indices

$fl$	Node with flexibility provider connected
$\Delta$	Node where the voltage constraint should be violated

### Variables

$p^g, q^g$	Real/reactive power generation
$p^d, q^d$	Real/reactive power demand
$p_{fl}$	Real power of a specific flexibility provider
$v = e + if$	Voltage in rectangular coordinates
$v = \sqrt{e^2 + f^2}$	Voltage magnitude
$p_{ij}, q_{ij}$	Real/reactive power flow

### Parameters

$Y = g + ib$	Line admittance
$a_p \in \{-1, 1\}$	Parameter used to define a search direction
$c$	Cost for flexibility service
$V^l, V^u$	Relaxed voltage bounds
$v^l, v^u$	Operational voltage bounds
$p^{gl(u)}, q^{gl(u)}$	Distributed generator real/reactive power generation bounds
$p^{dl(u)}, q^{dl(u)}$	Load real/reactive power demand bounds
$p_{fl}^{l(u)}, q_{fl}^{l(u)}$	Flexibility provider's real/reactive power bounds

### Other

$x$	a constant value
$x^u$	an upper bound
$x^l$	a lower bound

of flexibility that could potentially be provided, while convex restriction method could be overly conservative when determining range of permissible flexibility. The feasibility issue is addressed in [13], but it also assumes exact knowledge of nodal power injections.

When accounting for the variability of nodal power injections, most existing approaches are based on some form of multi-level or robust optimization framework [14,15] that are computationally expensive, unless certain techniques are used in order to circumvent the issue of non-convexity of the AC power flow equations. Methods based on stochastic programming, like the ones in [16], provide the DSO with information on probability of constraint violation, resulting in less conservative results. However, these methods rely on probability parameters and assumptions that are usually not readily available to the DSOs. Interpreting probabilistic results can also be an issue for DSOs accustomed to worst case scenario operational paradigm.

Lastly, the issue of fairness in flexibility provision remains, to the best of authors' knowledge, rather unexplored. As we discuss in the following section, the inherit coupling between different flexibility providers (FP) could result in conditions unfavorable both from disadvantaged FPs' and DSO's perspective. While this issue is recognized

by the authors in [17], the analysis is limited to a problem that stems from rather simplistic regulatory rules regarding flexibility provision.

The main contributions of this paper are as follows:

- An optimization based method for determining the amount of admissible nodal flexibility with regards to DN voltage constraints. The method minimizes the influence of one FP over others' capability of providing the same services and ensures feasibility of the entire range of determined flexibility,
- Demonstration of the method's ability to analyze flexibility provision under different network operational conditions,
- A principled approach to a problem of aggregating the flexibility to be offered to the TSO by multiple flexibility providers on a DN

The remainder of the paper is organized as follows. Section 2 provides a simple example in order to clarify the issues we are trying to solve. Section 3 provides a description of the method and discusses some important underlying assumptions. Section 4 demonstrates the effectiveness of the proposed solution on several DN case studies. Section 5 discusses flexibility provision by multiple FPs, while Section 6 concludes.

## 2. An illustrative example

Throughout the paper we focus on real power flexibility provision to simplify the problem and the notation. However, the framework can easily be extended to reactive power provision by the FP. Let us consider a simplified model of a distribution network, a modified version of a well known IEEE 33 bus test case from [18], which is shown in Fig. 1.

We assume FPs are connected to medium voltage nodes 12 and 18. For generality, we assume FP is able to alter its real power injection in both directions.

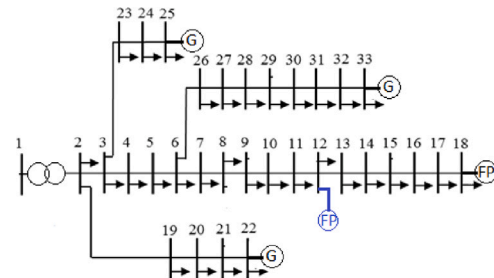
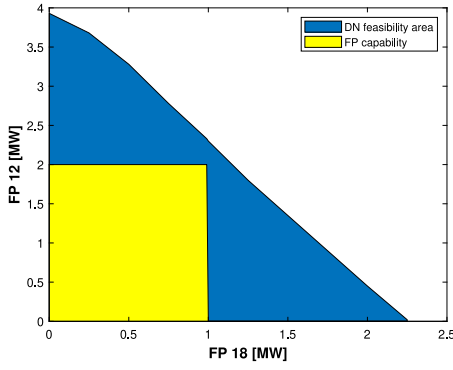


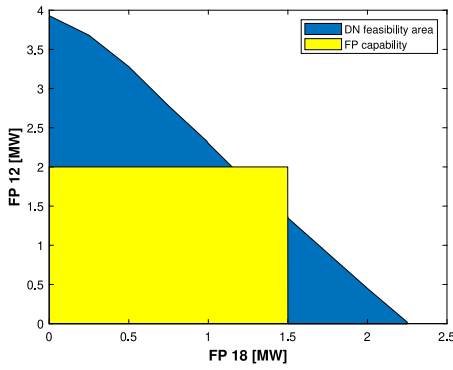
Fig. 1. Modified IEEE 33 bus distribution network test case.

The only real time measurements available are voltage and current at the substation (node 2). We determine the ranges of real and reactive power injections at every node, based on billing data, typical customer load profiles and DG historical data.

Given that the DN is of limited observability, we want to know the permissible range of real power (in any direction) of a *each individual* FP such that network voltage constraints will not be violated, regardless of the realization of nodal power injections. Furthermore, feasibility of the entire range of determined flexibility should be ensured. This means that any value of flexibility provision (within the determined range) will not result in violation of voltage constraints. In our example in Fig. 2(a) this would mean that the FP at node 18 should be able to provide any amount of flexibility between 0 and 1 MW without violating any DN voltage constraints. Since both FP at node 12 and 18 want to provide the flexibility service, the amount of flexibility determined for FP 18 should not be influenced by flexibility provision of FP 12. In other words, the amount of flexibility that can be provided should only be limited by voltage constraint violation caused primarily by a specific FP real power flexibility provision. Specifically, when we calculate the range of permissible flexibility of a FP connected to the node 12, we do not consider simultaneously the flexibility provision of a FP at node 18 and vice versa.



(a) Case where the capability area of each FP is a subarea of a distribution network feasibility area



(b) Case where the capability area of FPs is not entirely contained within distribution network feasibility area

Fig. 2. The relationship between distribution network feasibility area and a FP capability chart.

Next, let us consider only the case where the TSO wants to use the flexibility of FPs connected to the DN. The TSO can account for this flexibility by incorporating the entire DN into its calculations. However this could easily become intractable even if rough approximations are being used. Instead, it would be more efficient if the DSO provides only a bid structure (as, for example, shown by Fig. 8) of the available flexibility to the TSO. In this manner, the incorporation of the DN into TN is avoided. The problem here is the inherent impact that one FP could have on the ability of the other to provide the wanted amount of flexibility. The issue is best represented by Figs. 2(a) and 2(b).

There are two possible outcomes when calculating the maximum amount of flexibility each FP can provide. The first is the case where the capability area of a FP is contained within the feasibility area of a distribution network. In other words, there is enough headroom in the network so that every FP can provide the desired amount of flexibility without effecting other potential FPs. The maximum amount of flexibility that can be provided is the sum of individual FP power. The issue however, arises in the case represented by Fig. 2(b), where the vertex of a rectangle representing the sum of individual amounts of flexibility is located outside the feasibility area of the network. In this case, the bid structure must be formed, and communicated to the TSO, whereby no DN voltage constraints will be violated regardless of the amount or the source of flexibility activated. The obvious answer is to establish a price based merit order where the FP with the lowest price is first allowed to provide its desired amount of flexibility, and so on until there is no more DN headroom. However, this approach could potentially lead to low market liquidity in a case where FPs with lower bid price can only bid a smaller amount of flexibility. Hence we extend our method to show how it can be used to assess the impact of different merit orders on market liquidity.

### 3. Flexibility provision of a single FP

#### 3.1. Optimization problem formulation

In this section we provide a mathematical formulation of a optimization problem that constitutes a basis for the algorithm that is proposed for finding the range of permissible flexibility provision. Note here that presented optimization problem relies on assumptions that are discussed in detail in Section 3.3.

The formulation is based on a well known, non-linear optimal power flow (OPF) problem given in rectangular coordinates and real numbers by Eqs. (1)–(16).

$$\min p_{fl} \quad (1)$$

$$\sum_{(i,j) \in E \cup E^R} p_{ij} = p_i^g - p_i^d \quad \forall i \in N \quad (2)$$

$$\sum_{(i,j) \in E \cup E^R} q_{ij} = q_i^g - q_i^d \quad \forall i \in N \quad (3)$$

$$p_{ij} = g_{ij} v_i^2 - g_{ij}(e_i e_j + f_i f_j) + b_{ij}(f_i e_j - e_i f_j) \quad (4)$$

$$q_{ij} = -b_{ij} v_i^2 + b_{ij}(e_i e_j + f_i f_j) - g_{ij}(f_i e_j - e_i f_j) \quad (5)$$

$$p_{ji} = g_{ij} v_j^2 - g_{ij}(e_i e_j + f_i f_j) - b_{ij}(f_j e_i - e_j f_i) \quad (6)$$

$$q_{ji} = -b_{ij} v_j^2 + b_{ij}(e_i e_j + f_i f_j) - g_{ij}(f_j e_i - e_j f_i) \quad (7)$$

$$(V^l)^2 \leq e_i^2 + f_i^2 \leq (V^u)^2 \quad \forall i \in N \setminus N_{sl} \quad (8)$$

$$(v_{sl}^l)^2 \leq e_{sl}^2 + f_{sl}^2 \leq (v_{sl}^u)^2 \quad (9)$$

$$(v^u)^2 \leq e_d^2 + f_d^2 \leq (V^u)^2 \quad \forall \quad (10)$$

$$(V^l)^2 \leq e_d^2 + f_d^2 \leq (v^l)^2 \quad (11)$$

$$p_i^{gl} \leq p_i^g \leq p_i^{gu} \quad \forall i \in N_g \quad (12)$$

$$q_i^{gl} \leq q_i^g \leq q_i^{gu} \quad \forall i \in N_g \quad (13)$$

$$p_i^{dl} \leq p_i^d \leq p_i^{du} \quad \forall i \in N_d \quad (14)$$

$$q_i^{dl} \leq q_i^d \leq q_i^{du} \quad \forall i \in N_d \quad (15)$$

$$p_{fl}^l \leq p_{fl} \leq p_{fl}^u \quad (16)$$

$$q_{fl}^l \leq q_{fl} \leq q_{fl}^u \quad (16)$$

Eqs. (2)–(3) capture the active and reactive power balance. Eqs. (11)–(12) and (13)–(14) model the inherent variability of uncontrollable DGs and loads, respectively, as ranges of nodal power injections. Note that DGs are not flexibility providers, meaning their respective upper and lower bounds are derived based on historical data around some expected value, in the same manner the bounds are formed for loads. Although simplified, the formulation can easily be extended to accompany a more detailed DG models and operation modes (i.e. Volt-Var or power factor regulation). Eqs. (4)–(7) represent active and reactive power flows. FP real and reactive power constraints are given by (15)–(16). In general, these should reflect FP technical capabilities for flexibility provision, however, in certain cases, these constraints should be relaxed for the reasons discussed in Section 3.3. Eq. (8) constrains voltages between its relaxed limits  $V^u$  and  $V^l$ . Following the reasoning outlined in [10], in order to avoid restricting the feasible space of the problem, we let  $V^u$  and  $V^l$  be relaxed upper and lower voltage variable bounds, well outside of typical operational ranges for distribution networks.  $v^u$  and  $v^l$  are upper and lower voltage operating limits corresponding to the secure operating ranges which reflect power quality and safety requirements. Eq. (9) models voltage fluctuations at the substation as a continuous range rather than a fixed value. This range can be derived from voltage measurements that are usually readily available. Note here that, in the objective function, we assume FPs initial operating point to be zero, only for notational convenience.

The optimization procedure will set the most inconvenient values for substation voltage and power injection variables, reflecting a worst

case scenario with regards to flexibility provision. This is ensured by design, with a combination of a objective function and a constraint in (10).

There are two constraints of consideration in (10); the first one,  $(v^u)^2 \leq e_\Delta^2 + f_\Delta^2 \leq (V^u)^2$  forces the upper, while the second one,  $(V^l)^2 \leq e_\Delta^2 + f_\Delta^2 \leq (v^l)^2$  forces the lower operational voltage constraint of the node to be violated. The Eq. (10), in combination with an objective function in (1), forces the variables describing load and DG variability to purposefully violate voltage constraint at a specific node, denoted with  $\Delta$ . As there could exist more than one node with voltage constraint violation, the optimization method should be repeated, whereby a different node is selected as  $\Delta$ . Therefore, an iterative algorithm is developed and described in the following subsection.

### 3.2. Algorithm description

The iterative algorithm flow chart is shown in Fig. 3. For simplicity, we only show a step where upper voltage bound is violated. To impose lower voltage bound violation we substitute  $(v^u)^2 \leq e_\Delta^2 + f_\Delta^2 \leq (V^u)^2$  with  $(V^l)^2 \leq e_\Delta^2 + f_\Delta^2 \leq (v^l)^2$  and repeat the procedure.

The key steps of the algorithm are as follows:

Step 1: input network model parameters, specific network operating point and the bounds on demand, generation and FP variability. Set voltage constraint violation tolerance and FP node as a node on which the constraint from (10) will be forced upon.

Step 2: Solve the optimization problem from Section 3.1 with  $(v^u)^2 \leq e_\Delta^2 + f_\Delta^2 \leq (V^u)^2$  as (10)

Step 3: If the objective equals zero readjust the ranges of power injections and return to Step 1.

Step 4: If the problem is infeasible, then no voltage violations can occur — FP can provide flexibility within its entire range of technical capability.

Step 5: Check if there are upper voltage bounds violations on any other node in the network. If there are, set  $\Delta$  to an index of a node with the largest bound violation and return to Step 2. If there are no voltage bound violations, output the result.

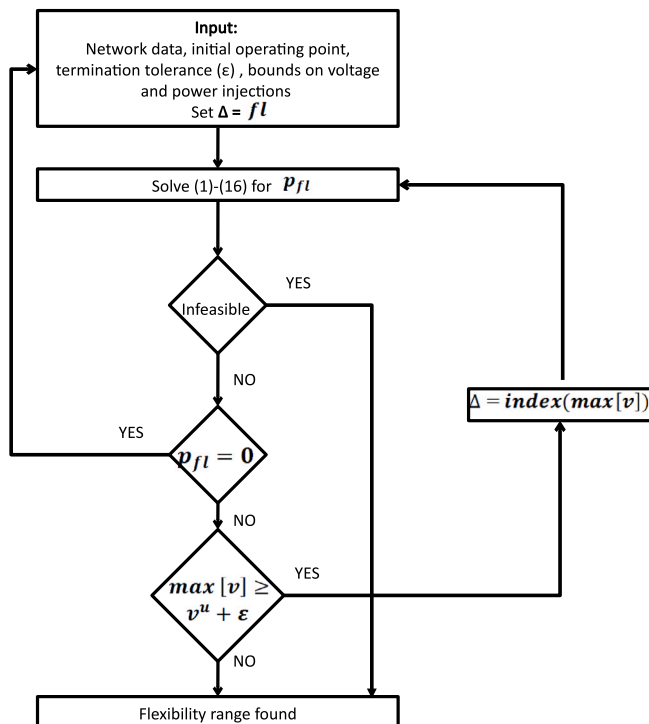


Fig. 3. Structure of the algorithm for permissible flexibility provision of a single FP.

### 3.3. Underlying assumptions and algorithmic performance

The algorithm relies on the assumption that there are no voltage violations in the network under normal operating conditions. This is not an unreasonable assumption, given that DSOs have to make sure no under or over voltage issues occur in every day network operation. The assumption implies that power and voltage ranges, provided as inputs, need to be set so they themselves cannot be the cause of any voltage violations and that violations are therefore caused only by the change in power injection of a specific FP. Given the lack of measurements, setting the ranges to satisfy this assumption could be difficult. However, the issue of non-compliance to this assumption is easily detectable. If the value of the objective function is zero, voltage bound is violated, even without any change in FP’s power injection, which is contrary to our initial assumption and input parameters should be reevaluated.

Secondly, the optimization problem in (1)–(16) could be infeasible. While, in general, this could be due to numerical issues, during our testing the issue always arose when the capability of a FP (meaning the range of available flexibility) was not sufficiently large enough to cause voltage violation. This issue is easily avoided by artificially increasing the range of flexibility of a specific FP in order to obtain a valid result. If the value of allowed flexibility surpasses the technical capabilities of a FP, the FP is constrained only by its technical capabilities in flexibility provision.

In order to avoid representing a problem as a mixed integer non-linear program, two versions of the algorithm are solved to find a lower and upper bound of flexibility. In most realistic cases, as our testing showed, the initial FP operating point is contained within these bounds (meaning we know the permissible range of flexibility in both directions). However, in general, there could exist a case where this is not true, meaning that it is possible to violate both lower and upper voltage constraints by changing the power of a FP in only one direction. In that case, one would only need to modify the objective function as in (17) in order to find the solution in a specific direction.

Finally, the method proposed could be considered robust (in a sense that for any realization of variable load and generation, voltage limits will not be violated) if the solution to the underlying optimization problem is a global one. Global, non-linear, off the shelf solvers can be used to provide a global solution to the optimization problem, however, their use could be prohibitive, mainly because of computational time required. Local solvers are faster and more reliable, but the robustness of the results cannot be guaranteed. Despite this, in a large number of real world networks, the local solution to an optimal power flow problem tends to also be the global one [19]. This was also the case in our extensive testing on several real world distribution networks. Since our optimization problem is structurally different from optimal power flow problem, further work is needed in order to study conditions where the local and global solution differ substantially and if certain recently developed methods as in [20–22] could alleviate the issue by providing the means of escaping from local solutions.

## 4. Numerical studies

In this section we first describe the methodology and test cases used to demonstrate the efficacy of the proposed method. We also extend our analysis in order to demonstrate the applicability of the proposed method in studying the impact of different ranges of power injection variability, as well as network reconfiguration on the range of permissible flexibility of a specific FP. Optimization problems are coded in MATLAB with YALMIP toolbox [23] and solved using the non-linear programming solver Ipopt [24]. Power flow simulations in Matpower [25] are used to verify the results.

**Table 1**  
IEEE 33 modified test case description.

# Nodes	# Lines	Subs. voltage range	DG nodes
33	32	0.98–1.02 p.u.	22,25,33
Load nodes	FP node	Base voltage	
2–33	12	12.66 kV	

4.1. Illustrative example using IEEE 33 bus test case

We consider a modified IEEE 33 bus test case with line parameters and nominal load as specified in [18] and shown by Fig. 1. We modify the test case by adding three DGs and one FP to nodes as specified by Table 1. DG nominal real power output is set to 1 MW. The range of voltage at the substation (node 2) is set to be between 0.98 and 1.02 p.u. We set the operating voltage limits,  $v^l$  and  $v^u$  to 0.9 and 1.1 p.u. respectively, and relaxed voltage limits,  $V^l$  and  $V^u$  to 0.7 and 1.3 p.u., respectively. The load and DG power injection ranges, representing the fluctuations around a nominal operating point, are parameterized in percentage of nominal values and are, for simplicity, the same for both loads and DG. We set the algorithm termination tolerance  $\epsilon$  (meaning a limit of voltage constraint violation) to  $10^{-5}$ .

4.1.1. Determining maximum flexibility for a FP connected to node 12

We assume  $\pm 5\%$  variation of base load real and reactive power and DG real power output. We also assume that FP can provide real power flexibility in both directions. Overall, the algorithm took 5 iterations, or approximately 5 s on a modest portable PC. Ipopt reports computational time in order of tenth of a second per iteration.

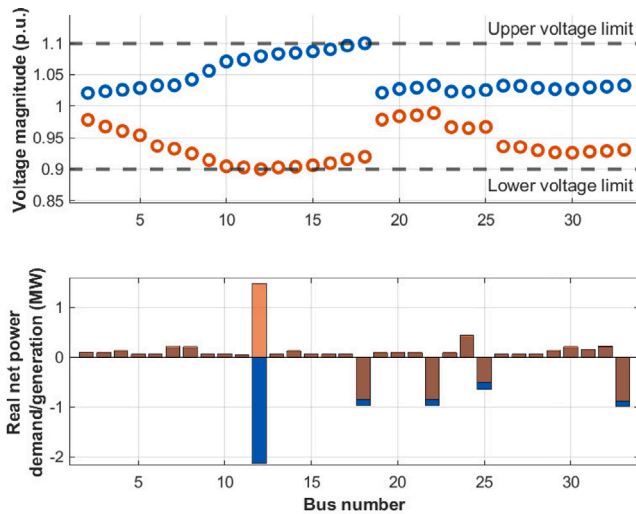


Fig. 4. Voltage profile of a DN test system with  $\pm 5\%$  variation in load and DG real and reactive power. Circles represent maximum (blue) and minimum (orange) voltage magnitude in each node in DN. Real power injections at each node match the nodal voltage profile above. Voltage profile depicted with orange circles is a result of nodal power injections represented by orange columns. The same applies to blue color columns.

Fig. 4 shows the maximum allowable real power injection for a FP at node 12 (bottom plot) whereby the voltage magnitude constraints are violated only within a set tolerance ( $\epsilon$ ). As shown in upper plot, this violation occurs at node 18 for upper operational voltage constraint, by which the net real power injection at node 12 is 2.19 MW, and at node 12 for a lower voltage constraint, by which the net real power demand at node 12 is 1.41 MW. The bottom plot also shows that the algorithm decreases the real power consumption of the loads and increases DG real power injection when trying to violate upper voltage constraint, and vice versa when trying to violate lower voltage constraints.

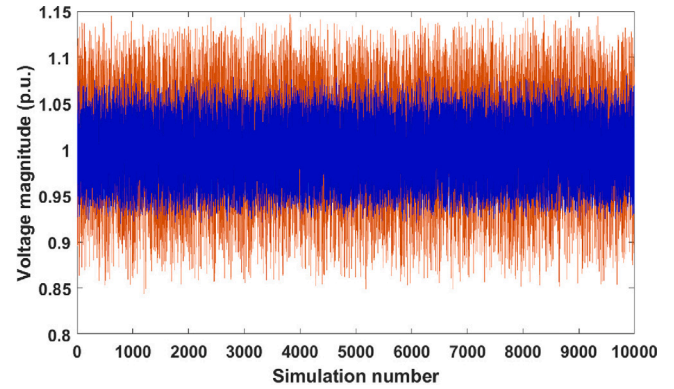


Fig. 5. Output of 10,000 Matpower load flow tests showing voltage magnitude for each of 33 buses in the test network. Orange color represents voltage magnitudes in case where variability is not considered, while blue color represents magnitudes where the power injection variability is considered.

To showcase the advantages of the proposed approach, we compare two test cases — one where no power injection or substation voltage variability is considered and the one where these variations are taken into consideration by using the proposed method. In the former case, bounds on flexibility are calculated by solving a typical OPF where the objective is to maximize (minimize) the amount of available flexibility for a specific FP, while load and DG power injections are set to their nominal values and substation voltage is set to 1 p.u. <sup>1</sup>

In this case the range of permissible flexibility at FP 12 is between  $-2.29$  MW to  $3.23$  MW. In the latter case, we assume  $\pm 20\%$  variation of base load real and reactive power and  $\pm 10\%$  variation in DG real power output. The range of voltage at the substation (node 2) is set to be between 0.94 and 1.06 p.u. In this case we determined permissible range of flexibility at FP 12 to be between  $-0.6$  MW to  $0.94$  MW.

We proceed by computing 10,000 power flows in Matpower for both cases separately. We generate random load and DG nodal power injections as well as substation voltage within the aforementioned ranges, while real power of a FP at node 12 is generated randomly within ranges determined with each of the two cases' respective method. The results of these simulations are shown in Fig. 5. As shown, ignoring the inherent variability significantly increases the probability of nodal voltage constraint violations.

4.1.2. Impact of nodal power injection variability

In this subsection we demonstrate the applicability of the proposed framework to studying the effect of load and DG variability to the permissible flexibility provision. We increase the load and DG power injection variability to  $\pm 25\%$ . All other parameters are the same as in Section 4.1.1. Fig. 6 shows the results in the same manner as Fig. 4.

The maximum permissible flexibility of a FP connected to node 12 is now reduced significantly: from 2.19 MW to 1.23 MW of power production, and from 1.41 MW to 0.74 MW of power consumption. For a 20% increase in variability, there is approximately 50% reduction in permissible flexibility. Remember that the ranges of power injections represent the fluctuations around some nominal operating point. These ranges are only estimated based on available data sources. By increasing the number of available measurements, these ranges could be further reduced. As the exercise demonstrates, this reduction would lead to a significant increase in permissible flexibility provision.

<sup>1</sup> While other, more sophisticated approaches exist, we use a rather naive one, primarily in order to emphasize the effect that neglecting variability has on voltage constraint violation

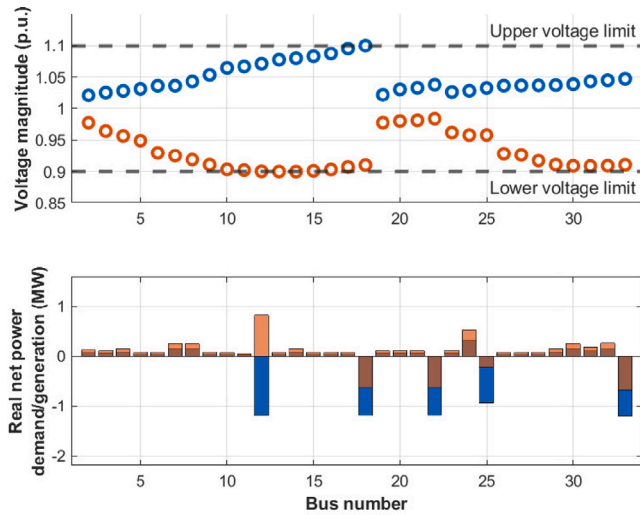


Fig. 6. Voltage profile of a DN test system with  $\pm 25\%$  variation in load and DG real and reactive power. Circles represent maximum (blue) and minimum (orange) voltage magnitude in each node in DN. Real power injections at each node match the nodal voltage profile above. Voltage profile depicted with orange circles is a result of nodal power injections represented by orange columns. The same applies to blue color columns. Compared to a base case from Fig. 4 there is a substantial reduction in amount of permissible flexibility at node 12.

#### 4.1.3. Impact of network reconfiguration

In order to illustrate the effect of network reconfiguration to the range of permissible flexibility provision, we connect the nodes 18 and 33, thereby changing the topology of the DN from radial to weakly meshed one. We again run the algorithm and compare the results to the base case (as shown in Fig. 4), by again setting all the parameters to values from Section 4.1.1. The results are shown by Fig. 7.

We observe that changing the topology resulted in substantial increase of range of permissible flexibility, at least in real power production direction — from 2.19 MW to 3.64 MW. While the change is substantial in this example, in general it is highly dependent on the specific connections and line parameters. However, this exercise shows that the proposed method could be used to assess the effect of certain control options that are at the DSO’s disposal, on the range of permissible flexibility.

Finally, note here that, the flexibility provision could also be viewed as a node hosting capacity, meaning that the proposed method could also be used to determine the maximum amount of generation or demand that could be connected to a specific node in DN.

#### 4.2. Numerical studies using the real world distribution network test cases

Finally, we show the effectiveness of our algorithm using the real world distribution network test cases from Croatia [26], UK [27] and Portugal [28]. Unlike the simplistic IEEE 33 test case, the networks used here are more complex with regards to modeling (containing lines with shunt impedance, transformers with tap changers and capacitor banks), size, and topology. Some of the properties of these networks are shown in Table 2.

Table 2  
Real world distribution network test cases.

Test case	# Nodes	# Lines/Transf.	Slack volt. range p.u.	DG nodes	Base voltage
Croatia	22	34	0.94–1.06	14	110/35 kV
Portugal	229	229	0.93–1.07	18,114,221	15/30/60 kV
Rural UK	66	66	0.98–1.02	19,23,40	6.6 kV

We set the variability of load and DG nodal power injections to  $\pm 10\%$  and  $\pm 20\%$  respectively. Voltage range at substation node is shown

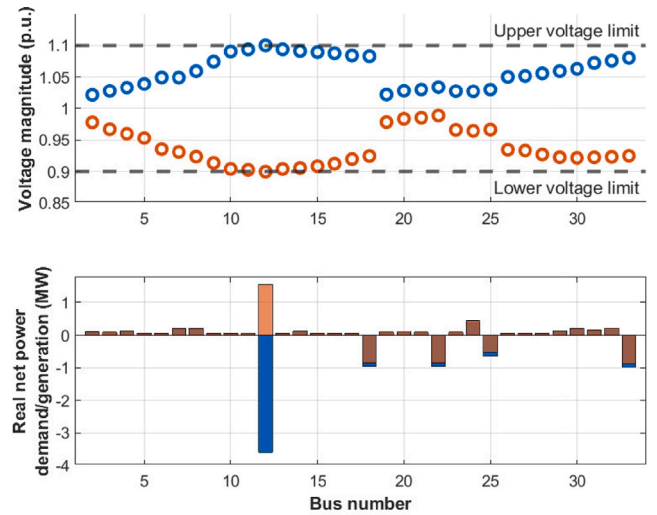


Fig. 7. Voltage profile of a DN test system with  $\pm 5\%$  variation in load and DG real and reactive power. Circles represent maximum (blue) and minimum (orange) voltage magnitude in each node in DN. Real power injections at each node match the nodal voltage profile above. Voltage profile depicted with orange circles is a result of nodal power injections represented by orange columns. The same applies to blue color columns. Compared to a base case from Fig. 4 there is a substantial increase in amount of flexibility at node 12 simply as a result of altering the topology of the network.

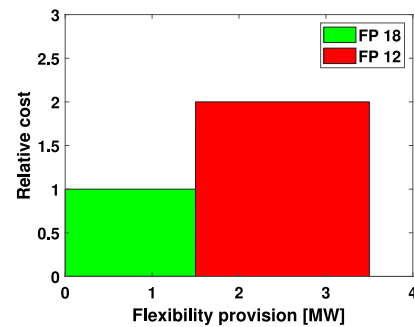


Fig. 8. A simplified example of FP’s bid price structure.

in Table 2. The range of operating voltage limits is 0.94–1.06 p.u. for Rural UK test case and 0.9–1.1 p.u. for the rest. Unlike in the previous test case, where we computed flexibility range for one FP at a specific node, here the real power flexibility range is determined for every node in the network. Again, we compute 10,000 load flow simulations to assess the quality of our solution.

Table 3  
Results of the real world DN test cases.

Test case	Max numb. of voltage violations	Max numb. of iterations	Max algorithm comp. time [s]
Croatia	0	7	15.25
Portugal	0	7	450.3
Rural UK	0	11	80.4

The results of our simulations are presented in Table 3. Since simulations are conducted for every node in the network, we show only the maximum value of specific metrics that best represent the quality of the solution. The computational time metric encompasses both solver time and preprocessing. On all test cases, solver time is usually an order of magnitude lower than time spent on preprocessing, ranging from under 1 s for Croatia and UK network, to under 10 s per iteration in case of much larger, Portuguese test case. The effectiveness of our approach is demonstrated by the fact that there were no voltage constraint violations for any of 317 nodes tested in total.

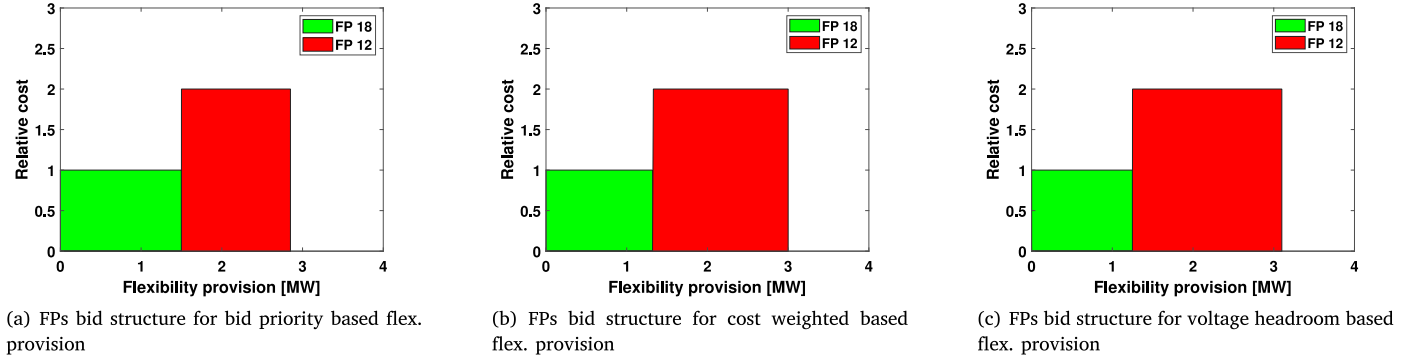


Fig. 9. Bid structures for FPs in nodes 12 and 18. Figures progressively show how different flexibility provision assessment schemes result in an increase in overall market liquidity.

## 5. Extending the framework to overall DN flexibility assessment

So far, we have been focused on determining the flexibility provision of a single FP. In what follows, we discuss the problem of aggregating this flexibility from multiple providers.

Let us again consider an example from Fig. 2(b). By applying the proposed algorithm, we determine the permissible flexibility provision from FP 18 and FP 12 to be 1.5 MW and 2 MW respectively. Now let us consider bids for flexibility provision for these two FPs as presented by Fig. 8, where both FPs bid their respective maximum amount of permissible flexibility. Note that we assume FP's flexibility capability area is a superset of what is constrained by network voltage violation. This bid price structure cannot be communicated to the market operator since the overall flexibility of 3.5 MW cannot be achieved without network voltage constraint violation, as shown by Fig. 2(b). An obvious solution would be to allow FP 18 bid its maximum amount of flexibility, reason being its lower price bid, and then to calculate FP 12 maximum while keeping FP 18 fixed to its maximum value. However, in doing so, we have decreased market liquidity since the overall amount of flexibility is reduced when compared to a case where FP 12 flexibility is at its maximum. We address the issue of trade off between cost minimization and market liquidity by developing three different flexibility assessment schemes in the following subsections.

Note that the prices of flexibility used here are arbitrary and not given in specific units. Given that the focus here is to study the mutual impact of FPs, we are only interested in flexibility cost in relative terms.

### 5.1. Bid priority based flexibility provision

Given the known quantities of a bid, a merit order is established where the maximum amount of offered flexibility of a FP with the lowest bid is fixed and the proposed algorithm is used in order to find a maximum amount for the second FP. Once found, the procedure continues until the DN feasibility area boundary is reached. The main disadvantage of this approach is the case where the FP with the lowest bid is also the one closest to the feasibility boundary of a DN. In other words, the voltage violations in the network will occur for a small amount of flexibility provided by the FP with the lowest bid. This reduces the amount of flexibility other FPs could potentially provide, hence reducing the overall amount of flexibility that could be provided. The resulting bid structure is shown by Fig. 9(a). FP at node 18 is allowed to provide its maximum flexibility, while FP at node 12 is curtailed because of the lack of voltage headroom. In this case the overall flexibility amount is the smallest of three cases presented.

### 5.2. Cost weighted flexibility provision

In this case we want to reduce the impact of specific FP on overall liquidity by finding the appropriate middle ground between overall

cost and the available flexibility. This is accomplished by modifying the problem in the following manner. The objective function in (1) is replaced by the following expression:

$$\min a_p \sum_{fl} p_{fl} \quad (17)$$

with  $a_p$  ensuring all FPs provide power in the same direction. Additional constraints that couple flexibility amount of different FPs are introduced:

$$c_i p_i = c_{i+1} p_{i+1} \quad \forall i \in N_{fl} \quad (18)$$

These constraints are added in order to weigh the amount of flexibility provision from each FP based on its cost ( $c$ ) offered for the service. The resulting bid structure is shown by Fig. 9(b). Flexibility provision of FP 18 is curtailed, but the overall flexibility amount is increased.

### 5.3. Voltage headroom weighted flexibility provision

In this case we want to again increase the overall liquidity based on voltage headroom available to the FP. In other words, we favor the flexibility provision of an FP that can provide more flexibility before it violates voltage constraints of the network. This is accomplished again by defining the objective function as in (17), while instead of (18) the additional constraints become:

$$p_i^u p_i = p_{i+1}^u p_{i+1} \quad \forall i \in N_{fl} \quad (19)$$

This means that flexibility provision of each FP is weighted according to its maximum flexibility capability as determined by the method in the first step. The resulting bid structure is shown by Fig. 9(c). Flexibility provision of FP 18 is again curtailed but the overall flexibility availability is the highest among the three proposed schemes.

## 6. Conclusion

We have proposed a deterministic, optimization based method that is able to resolve some of the less obvious issues with flexibility provision at the DN level. The DSO can use the method to pre-detect the range of permissible flexibility while accounting for inherent power injection and voltage variability. The specific combination of objective function and constraints of the underlying optimization method ensures the feasibility for the entire range of permissible flexibility as well as no voltage constraint violations can occur for any combination of power injections (within the specified range). The initial assumptions that the method relies upon are discussed. We first demonstrated the effectiveness of the method on a simple DN where we have shown different effects of variability and grid topology on the range of permissible flexibility. The analysis shows that reducing the estimated range of power injections as well as making changes in topology leads to substantial increase in permissible range of flexibility. This has further

practical implications for the DSO as the problem at hand could also be used for assessing grid hosting capacity. We have extended our testing to three real world DNs to further demonstrate the efficacy of the proposed method. In all test cases, no voltage constraint violations occurred for any of 317 nodes tested.

We next discussed the issue of having multiple FPs on the same DN and the effect they have on each other when competing for providing the flexibility service. We showed that the proposed framework could easily be extended, by simply incorporating specific additional constraints, to provide a more favorable outcome in terms of increase in overall amount of flexibility.

### CRedit authorship contribution statement

**Martin Bolfek:** Conceptualization, Methodology, Formal analysis, Writing – original draft, Visualization. **Tomislav Capuder:** Writing – review & editing, Validation, Supervision, Funding acquisition.

### Declaration of competing interest

One or more of the authors of this paper have disclosed potential or pertinent conflicts of interest, which may include receipt of payment, either direct or indirect, institutional support, or association with an entity in the biomedical field which may be perceived to have potential conflict of interest with this work. For full disclosure statements refer to <https://doi.org/10.1016/j.epr.2022.108262>. Martin Bolfek reports financial support was provided by Innovation and Networks Executive Agency (INEA).

### Acknowledgments

The research leading to these results has received funding from the European Union's Horizon 2020 research and innovation programme under Grant Agreement No. 864298 (project ATTEST). The sole responsibility for the content of this document lies with the authors. It does not necessarily reflect the opinion of the Innovation and Networks Executive Agency (INEA) or the European Commission (EC). INEA or the EC are not responsible for any use that may be made of the information contained therein.

The work is supported by Croatian Science Foundation (HRZZ) and Croatian Distribution System Operator (HEP ODS) through project IMAGINE - Innovative Modelling and Laboratory Tested Solutions for Next Generation of Distribution Networks (PAR-2018).

### References

- Matevosyan, Julia and Giannakidis, George and Joyeau, Alban and Gómez Simon, Cristina and Lallemand, Mathilde and Martin, Alastair and Anisie, Arina and Marquant, Julien and Gutiérrez, Laura and Sani, Lorenzo and Janeiro, Luis and Komor, Paul and Miranda, Raul and Collins, Sean, Demand-Side Flexibility for Power Sector Transformation, Tech. Rep., 2019, pp. 1–44, [Online]. Available: [www.irena.org](http://www.irena.org).
- D. Tong, D.J. Farnham, L. Duan, Q. Zhang, N.S. Lewis, K. Caldeira, S.J. Davis, Geophysical constraints on the reliability of solar and wind power worldwide, *Nature Commun.* 12 (1) (2021) 6146, [Online]. Available: <https://www.nature.com/articles/s41467-021-26355-z>.
- G. Pretticco, A. Vitiello, Distribution System Operator Observatory 2020, Tech. Rep. KJ-NA-30561-EN-N (online), KJ-NA-30561-EN-C (print), Publications Office of the European Union, Luxembourg (Luxembourg), 2020, [Online]. Available: <https://ec.europa.eu/jrc>.
- D.M. Gonzalez, J. Myrzik, C. Rehtanz, The smart power cell concept: Mastering TSO-DSO interactions for the secure and efficient operation of future power systems, *IET Gener., Transm. Distrib.* 14 (13) (2020) 2407–2418.
- X. Jin, Y. Mu, H. Jia, Q. Wu, T. Jiang, M. Wang, X. Yu, Y. Lu, Alleviation of overloads in transmission network: A multi-level framework using the capability from active distribution network, *Int. J. Electr. Power Energy Syst.* 112 (2019) 232–251, [Online]. Available: <http://www.sciencedirect.com/science/article/pii/S0142061519305137>.
- S. Riaz, P. Mancarella, Modelling and characterisation of flexibility from distributed energy resources, *IEEE Trans. Power Syst.* 37 (1) (2022) 38–50.
- P. Fortenbacher, T. Demiray, Reduced and aggregated distribution grid representations approximated by polyhedral sets, *Int. J. Electr. Power Energy Syst.* 117 (2020) 105668, [Online]. Available: <http://www.sciencedirect.com/science/article/pii/S0142061519309159>.
- M. Kalantar-Neyestanaki, F. Sossan, M. Bozorg, R. Cherkaoui, Characterizing the reserve Provision Capability Area of active distribution networks: A linear robust optimization method, *IEEE Trans. Smart Grid* 11 (3) (2020) 2464–2475.
- M. Bolfek, T. Capuder, An analysis of optimal power flow based formulations regarding DSO-TSO flexibility provision, *Int. J. Electr. Power Energy Syst.* (2021).
- D.K. Molzahn, L.A. Roald, Grid-aware versus grid-agnostic distribution system control: A method for certifying engineering constraint satisfaction, in: *Proceedings of the Annual Hawaii International Conference on System Sciences*, Vol. 2019-Janua, 2019, pp. 3445–3454.
- S.C. Ross, J.L. Mathieu, A method for ensuring a load aggregator's power deviations are safe for distribution networks, *Electr. Power Syst. Res.* 189 (2020).
- D. Lee, K. Turitsyn, D.K. Molzahn, L. Roald, Robust AC optimal power flow with robust convex restriction, *IEEE Trans. Power Syst.* (2021).
- N. Nazir, M. Almassalkhi, Convex inner approximation of the feeder hosting capacity limits on dispatchable demand, in: *Proceedings of the IEEE Conference on Decision and Control*, Vol. 2019-Decem, 2019, pp. 4858–4864.
- S. Zhou, Y. Zhao, W. Gu, Z. Wu, Y. Li, Z. Qian, Y. Ji, Robust energy management in active distribution systems considering temporal and spatial correlation, *IEEE Access* 7 (2019) 153635–153649.
- X. Zeng, H. Wu, M. Ding, R. Bi, B. Xu, J. Ding, Two-stage robust optimization for practical reactive power in distribution network based on multiple constraint convex approximation, *Int. J. Electr. Power Energy Syst.* 134 (2022).
- V.A. Evangelopoulos, I.I. Avramidis, P.S. Georgilakis, Flexibility services management under uncertainties for power distribution systems: Stochastic scheduling and predictive real-time dispatch, *IEEE Access* 8 (2020) 38855–38871.
- K. Petrou, M.Z. Liu, A.T. Procopiou, L.F. Ochoa, J. Theunissen, J. Harding, Operating envelopes for prosumers in LV networks: A weighted proportional fairness approach, in: *IEEE PES Innovative Smart Grid Technologies Conference Europe*, Vol. 2020-October, 2020, pp. 579–583.
- A. Wazir, N. Arbab, Analysis and optimization of IEEE 33 bus radial distributed system using optimization algorithm, *Jetae* 1 (2) (2016) 2518–4059, [Online]. Available: <http://inu.edu.pk/Vol1No2/JETAe-01-02-07.pdf>.
- W.A. Bukhsh, A. Grothey, K.I.M. McKinnon, P.A. Trodden, Local solutions of the optimal power flow problem, *IEEE Trans. Power Syst.* 28 (4) (2013) 4780–4788, [Online]. Available: <http://ieeexplore.ieee.org/document/6581918/>.
- N. Costilla-Enriquez, Y. Weng, B. Zhang, Combining Newton-raphson and stochastic gradient descent for power flow analysis, *IEEE Trans. Power Syst.* 36 (1) (2021) 514–517.
- Y. Tang, S. Low, Distributed algorithm for time-varying optimal power flow, in: *2017 IEEE 56th Annual Conference on Decision and Control*, Vol. 2018-Janua, CDC, IEEE, 2017, pp. 3264–3270, [Online]. Available: <http://ieeexplore.ieee.org/document/8264138/>.
- L. Zhang, B. Zhang, An iterative approach to improving solution quality for AC optimal power flow problems, 2021, [Online]. Available: <http://arxiv.org/abs/2109.06356>.
- J. Löfberg, YALMIP: A toolbox for modeling and optimization in MATLAB, in: *Proceedings of the IEEE International Symposium on Computer-Aided Control System Design*, 2004, pp. 284–289.
- A. Wächter, L.T. Biegler, On the implementation of an interior-point filter line-search algorithm for large-scale nonlinear programming, *Math. Program.* 106 (1) (2006) 25–57.
- R.D. Zimmerman, C.E. Murillo-Sánchez, R.J. Thomas, MATPOWER: Steady-state operations, planning, and analysis tools for power systems research and education, *IEEE Trans. Power Syst.* 26 (1) (2011) 12–19.
- M. Bolfek, Daily profiles (2020) of load of a electricity distribution network (40 nodes) from Croatia – ATTEST project, 2022, <http://dx.doi.org/10.25747/z9qp-8d97>.
- E. Martinez-Ceseña, W. Kong, Daily profiles (2020) of load of a rural synthetic electricity distribution network from UK – ATTEST project, 2022, <http://dx.doi.org/10.25747/rfde-c940>.
- N. Fonseca, H. Teixeira, F. Ribeiro, A. Madureira, F. Soares, Daily profiles (2020) of load and generation of a semi-urban electricity distribution network from Portugal – ATTEST project, 2022, <http://dx.doi.org/10.25747/5fhk-gn76>.